ELSEVIER

New practical algorithm for modelling retention times in gradient reversed-phase high-performance liquid chromatography

G. Hendriks [a,*], J.P. Franke [b], D.R.A. Uges [c]

[a] *Pharma Bio-Research Group BV, P.O. Box 200 9407AE Zuidlaren, The Netherlands*
[b] *Department of Pharmaceutical Analysis, University Centre Pharmacy, P.O. Box 196 9700 AD Groningen, The Netherlands*
[c] *Laboratory for Drug Analysis and Toxicology, Department of Pharmacy, Groningen University Hospital,*
P.O. Box 30.000 9700 RB Groningen, The Netherlands

Abstract

Computer models have been widely used to predict the chromatographic behaviour of liquid chromatography systems. With the introduction of mass spectrometric detection and the use of lower mobile phase flow rates with conventional LC equipment, the influence of the dwell volume on the shape of the gradient curve becomes an issue in predicting the retention times. A new straight forward algorithm is proposed for the modelling of retention times in reversed-phase LC, taking the effect of the dwell volume on the gradient shape into account. The results show that the dwell volume has a large effect at lower flow rates and on the retention times of the analytes eluting at the end of fast gradient curves. The proposed model is able to make reliable predictions and can be helpful in LC–MS method development.
© 2005 Elsevier B.V. All rights reserved.

Keywords: Computer simulation; Mobile phase composition; Gradient elution; Retention times; Dwell volume; Algorithm; Modelling; LC–MS

1. Introduction

Computer models describing LC systems are helpful for understanding the behaviour of the LC system and can speed-up method development. Various publications describe the use of a computer program during LC method development and optimisation [1–3,8,10]. DryLab is probably the best known [1]. This powerful software is able to predict retention times under isocratic and gradient conditions. The development and functionalities are well described by Molnar [1]. Longxing et al. [8] proposed a uniform algorithm to predict retention times during gradient elution. It produces excellent predictions but it takes several minutes to perform a calculation of one analyte on a general personal computer.

In the past decade the mass spectrometric detector, MS, is much more used routinely. As a result of its high selec-tivity, chromatographic resolution is much less of a problem and chromatographic runtimes could be shortened. However, there are several reasons for separating analytes and non-analytes because they can interfere with each other during the ionisation process in the mass spectrometer, which will result in inaccurate detector responses [7]. There was also a tendency to lower column diameters to gain sensitivity and to reduce the LC flow rate into the MS. Fast gradient conditions are used to speed up the analysis time [7].

As a result of the internal LC-system volume, the shape of the originally programmed gradient becomes much more affected by the dwell volume as the eluent flow decreases and the gradient time is held constant. This is the case when scaling down the internal column diameter [5,13,15,16]. Although the dwell volume is taken into account in the before mentioned prediction models, the deteriorated shape of the gradient curve is not taken into account in predicting retention times.

As a consequence, the use of fast analyses with narrow bore columns and conventional LC equipment leads to errors

---

* Corresponding author. Tel.: +31 592 303477; fax: +31 592 303223.
E-mail address: ghendriks@pbr.nl (G. Hendriks).

in the prediction of retention times under gradient conditions due to the internal system volume [16].

In this paper a universal and fast algorithm is proposed to model a reversed-phase LC-system based on general LC theory.

Because of multiple sequential calculation steps that are needed and due to the nature of our calculations, we preferred a discontinuous algorithm to keep the overview over the calculation process. A continuous method should lead to an iterative method.

The starting point is a relationship between the modifier concentration and the linear velocity of the analyte band on the column. The goal was to estimate the modifier concentration in the direct vicinity of the analyte band during gradient elution. Therefore, a calculation method was set up to determine the actual shape of the gradient curve. The programmed gradient curve is corrected for time shifts due to the system volume and for the increasing migration distance of the analyte band on the column. The shape of the programmed gradient curve is corrected for the influence of dead volumes by a proposed semi empirical model. The retention time is calculated by a discontinuous calculation process where the time from the injection is repeatedly increased by a small time period. During each period the modifier concentration in the vicinity of the analyte band is calculated and subsequently the linear velocity of that band. The time increments and the migration distances are summarised until the total migration distance equals the column length and the band is said to be eluted. The retention time is now equal to the sum of the time increments.

This calculation method leads to more accurate predictions when fast gradient conditions are used on conventional LC equipment at lower flow rates. The proposed model is able to predict retention times under isocratic and (multi period) gradient conditions. It is also able to predict the actual column effluent composition at any time. This can be helpful as the eluent composition affects not only the retention times of the analytes but also their ionisation in the MS interface [11].

Using this model, good estimations of retention times are made with a minimum of experimental effort.

2. Theory

The goal of our method is to determine the actual mobile phase composition in the direct vicinity of the centre of the analyte band at any time during a chromatographic run. Once we have established this composition, the actual velocity of the analyte in the column is calculated and from that velocity the distance migrated within a finite period of time can be calculated. This process is repeated until the total migration distance is equal to the length of the column as the analyte is said to be eluted.

To set up this band tracking model (BT-model) we divided the whole procedure in four parts.

(1) Finding a suitable equation to model the relationship between the modifier concentration and the capacity factor of the peaks of interest.
(2) Set up an equation to determine the speed of the bands on the column as a function of the modifier concentration.
(3) Developing a calculation method for the determination of the actual modifier concentration at the centre of the analyte band during gradient elution, based on the programmed gradient curve and taking gradient curve distortion into account.
(4) Tracking the bands during the chromatographic progress.

2.1. Retention parameters

The first issue in modelling a chromatographic separation is to determine the relationship between the capacity factor, k, and the modifier concentration, φ. In 1976, Horváth et al. [6] introduced a relationship based on the solvophobic theory. This model is probably one of the best but it is hard to fit the curve from experimental data because of the many parameters. For isocratic runs an equation of straight line as given in Eq. (1) can be found in many textbooks and is the base of many modelling algorithms.

$$\ln k = A\varphi + B \tag{1}$$

Eq. (1) is most convenient but some combinations of compounds and modifiers used in mobile phases result in curved relationships [9]. This phenomenon is often present when acetonitrile is used as a modifier [8,12]. As acetonitrile is a widely used modifier, we choose Eq. (2) as a general estimate to describe the relationship between k and φ [8,9,12].

$$\ln k = A\varphi^2 + B\varphi + C \tag{2}$$

This model is easy to fit by straight forward linear regression. It needs at least three isocratic experiments at three different modifier concentrations and a determination of the dead time, t_0, in order to calculate the capacity factor according to Eq. (5).

2.2. From modifier concentration to linear velocity

To calculate the velocity of a band we derived an equation to express the capacity factor in terms of linear velocity.

We expressed the linear velocity of the mobile phase, v_0, in terms of column length, L, and the dead time, t_0, by:

$$v_0 = \frac{L}{t_0} \tag{3}$$

and the linear velocity, v_i, of an analyte, i, as:

$$v_i = \frac{L}{\mathrm{tr}_i} \tag{4}$$

where tr_i is the retention time of analyte i.

The capacity factor, k, is given by the generally used Eq. (5).

$$k_i = \frac{\mathrm{tr}_i - t_0}{t_0} \tag{5}$$

The capacity factor of a component i, can now be described as a function of the linear velocity, v_i, of the component by substituting Eqs. (3)–(5) for t_0 and tr_i, respectively.

$$k_i = \frac{v_0 - v_i}{v_i} \tag{6}$$

Then we rearranged Eq. (2) as:

$$\ln\left(\frac{v_0 - v_i}{v_i}\right) = A\varphi^2 + B\varphi + C \tag{7}$$

which gives for v_i:

$$v_i = \frac{v_0}{1 + e^{A\varphi^2 + B\varphi + C}} \tag{8}$$

Once the mobile phase composition in the vicinity of the analyte is known, its linear velocity on the column can be calculated by Eq. (8). In an isocratic system where the mobile phase composition remains constant, the retention time can be calculated in one step by dividing the column length, L, by its linear velocity, v_i, at a given modifier concentration, φ.

2.3. Determination of the actual modifier concentration at a given time

In gradient mode, the determination of the actual eluent composition in which the analyte is dissolved is more complicated. To solve this problem systematically, we had to find a suitable solution for three issues:

(1) Due to the dwell volume or hold up volume [4] it takes some time for the mobile phase composed by the gradient mixing system to reach the top of the column.
(2) The distance from the top of the column to the analyte is increasing during a chromatographic run.
(3) Due to the mixing effects of the dwell volume, the shape of the programmed gradient becomes deteriorated as shown in refs. [13,15,16].

For the calculation of the programmed modifier concentration at any given time we expressed the gradient table as programmed on a gradient LC system, as a data matrix containing the start time, t_{start}, the start composition φ_{start}, and the gradient slope, s, of all the periods in a programmed gradient table. The gradient slope is calculated by dividing the change of mobile phase composition, by the time of that particular period. From the corresponding period of this data set, the programmed mobile phase composition, φ, can be calculated at any time since the start of the chromatogram, t, during the chromatographic run by Eq. (9).

$$\varphi(t) = \varphi_{start} + s(t - t_{start}) \tag{9}$$
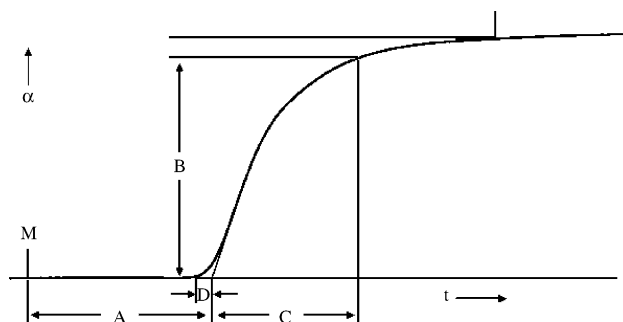

Fig. 1. Graphical determination of the system parameters. Example of a detector trace as can be observed when connecting an UV detector directly to the autosampler and a step gradient is programmed from a non-UV absorbing solvent to a solvent containing an UV absorbing agent. The programmed step gradient starts at mark M. The curve is manually extended by a tangent through the inflection point of the curve. Characters as explained in the text: (A) dwell time; (B) height, value of α, e.g. 0.9; (C) gradient time at $\alpha = B$; (D) time (between left side arrow and right side arrow) corresponding to $0.5 V_{avg}$.

2.3.1. Determining the dwell volume

The dwell volume can be determined graphically from a single experiment and should be determined for each configuration of the equipment as a system parameter [13].

A step gradient is run from a non-UV absorbing solvent, e.g. acetonitrile, to a solvent containing a certain amount of an UV absorbing agent as acetone or biphenyl at a concentration falling into the linear range of the detector.

The autosampler is connected directly to a UV detector and the trace is recorded at a suitable wavelength. A mark is placed on the recorder trace when the pump starts changing composition. An example of such a trace is shown in Fig. 1.

The dwell time, t_{dwell}, is the time from the mark to the front of the step in the trace to the front of the plateau of the graph, indicated as A in Fig. 1. The dwell volume, V_{dwell}, is now calculated by multiplying t_{dwell} by the mobile phase flow rate, F.

$$V_{dwell} = t_{dwell} F \tag{10}$$

2.3.2. Determining the "gradient delay in column"

The time the mobile phase needs to travel the distance from the top of the column to the analyte is sometimes called "gradient delay in column" [8].

We derived a calculation method that takes this continuously changing delay into account.

The time from the top of the column to the center of the analyte band (t_{corr}) is calculated from its distance, a_i, from the top of the column and the linear mobile phase velocity, v_0, by Eq. (11):

$$t_{corr} = \frac{a_i}{v_0} \tag{11}$$

2.3.3. Describing the actual gradient shape

The dead volumes of the LC system are responsible for a distortion of the shape of the programmed gradient [15,16].

This effect becomes more significant as the mobile phase flow decreases, the dwell volume increases and the slope of the gradient increases. Many user manuals of LC-pumps assume this disturbance as a symmetric S-shape and the dwell volume is measured from the start time of the gradient to the inflection point of the S-curve. The rounding of the gradient curve is described and discussed in detail [15,16]. For our model we needed a discontinuous method, so we derived a slightly different method to describe the actual shape of the gradient curve and incorporated it into the BT-model.

To describe the disturbance of the gradient curve we developed an semi empirical algorithm based on a two stage gradient profile disturbance. A one stage model did not describe the actual profile accurate enough. The resulting algorithm is a two-chamber disturbing model.

Although the effects of both chambers take place simultaneously in the physical LC system in the mixing chamber and the dead volumes in the system, the total effect is calculated as if the mobile phase passes a mixing chamber and a chamber where a general smoothing of the curve occurs. The combined effects of both chambers result in an accurate description of the gradient profile as it reaches the column. By splitting the effects, the calculation process becomes less complicated.

In the first chamber with a volume of V_d (dilution volume), the disturbance is only due to the mixing of two different eluent components. The effect is gained by diluting the actual eluent composition with the new composition as gradient mixing is in progress. When applying a step gradient to this chamber, the curve starts rising quickly but the slope decreases with time until the new programmed composition is reached. The decrease of this slope is directly related to V_d and the flow rate, F.

The effect of the second chamber is general smooth over the complete gradient curve after gradient mixing has occurred. The effect is reached by a moving average process. In this process a value in an array of numbers is recalculated as the average of that value and its surrounding values.

When only the second chamber is taken into account, a symmetrically shaped S-shaped curve is observed when a step gradient is applied to this chamber.

Fig. 2 shows the graphic representation of the effect of the two chamber model on a gradient profile programmed as a block gradient.

2.3.3.1. Determining V_d. The first chamber model which is mainly responsible for the deformation of the gradient curve at higher dwell volumes is thought to be a mixing/dilution chamber. A physical mixing chamber consists of parts of the actual gradient mixing chamber, the tubing and in low pressure gradient systems also the pump volume [13]. Actually, not the whole dwell volume contributes to the dilution effect as the total volume is not thoroughly mixed at any time but there is a continuous flow in and out. We preferred the name of dilution volume, V_d, over the name of mixing volume, V_m, which is reserved for a different calculation process [15,16].

In this model the disturbance of the gradient curve is thought of as a repetitive dilution of the mobile phase composition in the dilution chamber by the new mobile phase composition flowing into the chamber. The accuracy of the calculated dilution process, depends on the volume fraction of the chamber that is replaced with a new mobile phase composition, i.e. the dilution ratio. This ratio and the number of repetitive dilutions determine the progress of mixing during a change in eluent composition and an infinite number of dilutions indicate a complete replacement of the original mobile phase composition by the new one.

As the dilution process is a continuous process, the dilution ratio should be theoretically infinitely small but has a finite magnitude for use in our computerised model.

A one step gradient model is used to determine the dilution volume, V_d.

The proposed dilution chamber has a volume, V_d, containing a mobile phase composition φ_0. Any time period, Δt, a volume of mobile phase, $\Delta t. F$, with composition φ_1 flows into the chamber, the same volume with composition φ_0 flows out. The total volume of mobile phase in the chamber is mixed to composition φ. By repeating this process, φ converges to φ_1.

The dilution ratio can be calculated from the ratio of V_d and a fixed volume V_{res} which is the volume fraction that is replaced during Δt.

The number of repetitive dilutions (i.e. the number of Δt steps since the beginning of the process) is given by the total amount of mobile phase at a time, Ft, divided by V_{res}.

Eq. (12a) is derived from the described model, where α is the relative mobile phase composition indicating the fractional difference between φ_1 and φ_0.

$$\alpha = 1 - \left(\frac{V_d/V_{res} - 1}{V_d/V_{res}} \right)^{Ft/V_{res}} \tag{12a}$$

In a continuous dilution process V_{res} has an infinitely small value and α becomes:

$$\alpha = 1 - e^{-Ft/V_d} \tag{12b}$$

Evaluation of Eqs. (12a) and (12b) for values of V_{res}, indicated that a V_{res} value of less than 0.1 times V_d, leads to minor
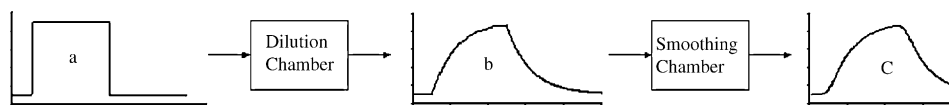

Fig. 2. Gradient curve deformation according to the two chamber model. A programmed block shaped change in mobile phase composition (a) is reshaped by the dilution chamber resulting in curve (b). The smoothing chamber rounds off the sharp edges of the curve (b) and results in the final curve (c).
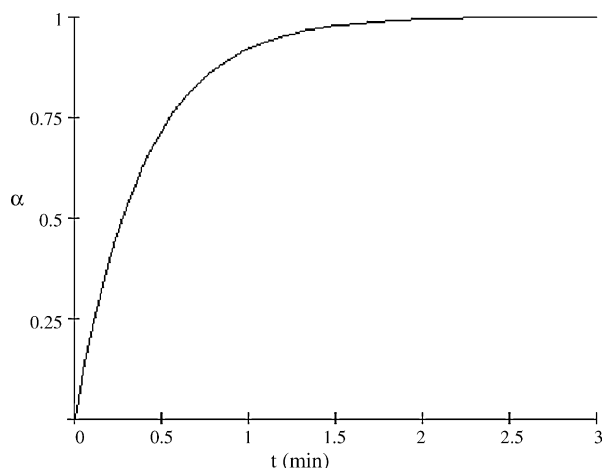
Fig. 3. Simulated dilution when a one step change in modifier concentration is applied to the dilution chamber with a volume of 0.2 ml at a flow 0.5 ml/min, according to Eq. (12b).

differences in the calculation of V_d. Our calculation model works, however, in a discontinuous time scale where the time is divided in small periods as will be seen later. This means that for the calculation of the dilution process in our model Eq. (12a) was applied.

Fig. 3 demonstrates the progress of step gradient calculated with a V_d of 0.2 ml, and at flow rate of 0.5 ml/min using Eq. (12b).

In Eq. (13), V_d is solved from Eq. (12b).

From a real detector trace, as described in Section 2.3.1, V_d can be determined by Eq. (13), at any combination of α and t at a given flow rate, F. An example is given in Fig. 1 where α and t are marked as B and C, respectively.

$$V_d(t, \alpha) = -\frac{Ft}{\ln(1 - \alpha)} \tag{13}$$

A determination at $\alpha = 0.9$ works well concerning the reading error of α and t from the detector trace and the smoothing effects, which diminishes at less steep parts of the curve. The latter will be discussed in Section 2.3.3.3.

2.3.3.2. Correcting the programmed gradient shape for V_d.
A real "disturbed" multi-period gradient profile is not easily described by one simple equation so we set up a discontinuous numerical method based on Eq. (12a).

Our starting point is the dilution chamber, as discussed in Section 2.3.3.1, with a volume V_d, containing a mobile phase with composition φ_0. During a finite period of time Δt, a volume $\Delta t. F$, of mobile phase with composition φ_n and flow F, flows into the chamber. Meanwhile a same volume with composition φ_0 flows out of the chamber to keep the content of the chamber at a constant volume. $\Delta t. F$ corresponds to V_{res} in Eq. (12a).

The new composition, φ, is determined by calculating the absolute amount of modifier flown into the chamber, $\Delta t. F\varphi_n$, summarized to the absolute amount of modifier already in the

vessel corrected for the flow out: $\varphi_0(V_d - \Delta tF)$. To calculate the concentration of the modifier the total amount of modifier is divided by V_d:

$$\varphi_t = \frac{\Delta tF\varphi_n + \varphi_0(V_d - \Delta tF)}{V_d} \tag{14}$$

For each Δt increment of time this procedure repeats where φ_0 is the previous modifier concentration and φ_n is the modifier concentration of the added flow.

2.3.3.3. The smoothing chamber model.
The second chamber of the disturbance model is a more hypothetical one. The physical basis of the second chamber is a combination of diffusion, and turbulent flow mixing in the dead volumes of the whole LC system. We found that the second chamber becomes of more importance when using high pressure gradient mixing systems with low volume mixing chambers. In this case a step gradient results in more regular S-shape which cannot be accurately described with the first mixing chamber.

The effect is modeled by a moving average smoothing method.

As will be seen in the next chapter, the gradient curve will be expressed and stored as a data matrix containing values for gradient time and the corresponding modifier concentration values.

Each value for modifier concentration is recalculated as a mean of its neighboring values, symmetrically distributed around the value to be recalculated. The volume corresponding to the range of these neighbouring values, i.e. the time range corresponding to the concentration values multiplied by the flow, is called the averaging volume, V_{avg}.

We choose the range of the neighboring values to correspond to a volume of $V_{avg}/7$ and repeated the recalculation process for seven times. This results in a smooth transition of fast concentration changes in the original gradient curve as is the case in a step gradient. The influence of the original data point decays to less than 1% at a distance of $0.5V_{avg}$ from that data point as the influence on the resulting curve works in both directions. In our model, V_{avg} is also treated as a system constant which means that it has to be determined once for a certain system configuration. This turned out to be a good assumption. V_{avg} can be determined as shown in Fig. 1. Distance "D" indicates the time corresponding to $0.5V_{avg}$. D is the time between the first change of the slope of the baseline to the point of intersection between the baseline and tangent through the inflection point of the curve. V_{avg} can be obtained from this time by multiplication with the flow rate, F. The tangent is used as an aid to distinguish the effect of V_d and V_{avg}.

2.3.3.4. The actual gradient curve.
The actual gradient curve as can be virtually observed at the top of the column, can now be calculated. The gradient curve is built by starting the total time, t, at 0 min and increasing it by Δt until the programmed end time is reached.

For each increment, the time, t, is corrected for the dwell time by Eq. (10) and the corresponding mobile phase composition is calculated by the matrix containing the gradient table using Eqs. (9) and (14).

The total gradient curve can be stored in a data matrix or table, containing the time, t, and the corresponding mobile phase composition. This gradient matrix is now subjected to the gradient distortion model. The resulting matrix contains the mobile phase composition at the top of the column at any time since the start of the gradient program at the pump.

2.3.4. The chromatographic progress

During the chromatographic progress the total runtime, t, is divided into small time periods, Δt as discussed earlier.

During the chromatographic run time the distance, a, from the top of the column to the centre of the analyte band is calculated for each increment of Δt.

As the analyte band migrates, the position of that band on the column is determined every period of Δt. At the moment of injection, at $t = 0$ and $a = 0$, the analyte is surrounded by a mobile phase with the start composition as indicated in the programmed gradient table. The actual linear velocity, v_i, is now calculated by Eq. (8) and the migration distance over the Δt period, Δa, is calculated by Eq. (15).

$$\Delta a = v_i \Delta t \tag{15}$$

The total chromatography time, t, is now increased by Δt and the total migration distance is increased by the calculated Δa.

From this position on the column a new mobile phase composition is determined by calculating a time point in the stored gradient curve matrix, t_{grad}, corrected for the traveled distance on the column using Eqs. (11) and (16) and taking the corresponding modifier concentration, φ:

$$t_{\text{grad}} = t - av_0 \tag{16}$$

When t_{grad} turns out to be negative, the analyte is still situated in the isocratic delay [4], i.e. the start composition.

With this new composition the whole process is repeated until the total distance, a, equals the column length. At this point the analyte is said to be eluted.

The retention time is now equal to t. This process is represented in the flowchart in Fig. 4.

Using this procedure the real average k, often referred as k^* [13], can be calculated as the momentary k value at the middle of the column, at $a = 0.5L$, by substituting the corresponding φ in Eq. (2).

The proposed procedures can be programmed in a spreadsheet program or another calculation sheet as Mathcad or Matlab (MathSoft, Cambridge, MA, USA).

We build a Windows based program with Delphi7. This program runs on a Pentium III 600 MHz personal computer and calculates the retention times of several components within a split second.
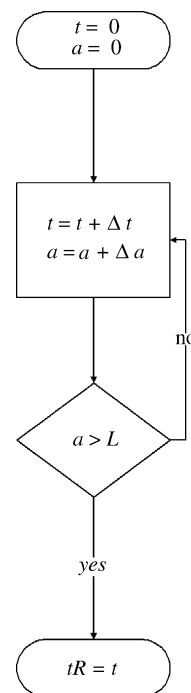

Fig. 4. The chromatographic progress: a, traveled distance of a chromatographic band; t, chromatogram time since the start of injection; L: column length; tr, predicted retention time; Δt, time increment; Δa, calculated distance during Δt.

3. Experimental

3.1. Materials

Digoxin (D3) and digoxigenin (D0) were purchased from Sigma (St. Louis, MO, USA). Digoxin monodigitoxoside (D1) and digoxin bisdigitoxoside (D2) were a generous gift of GlaxoSmithKline (Ware, UK). A test solution containing D0, D1, D2 and D3 was prepared in water:acetonitril (90:10, v/v) at a concentration of 500 ng/ml.

Acetonitril, HPLC grade, formic acid and sodium dihydrogen phosphate, analytical grade, were obtained from Merck (Darmstadt, Germany). Ultra pure water was obtained by using a Milli-Q water purification system (Millipore, Bedford, MA, USA).

3.2. Equipment

Chromatographic analyses were performed on a system with a low pressure gradient mixer. The system consisted of an Alliance 2690 separation module equipped with a column heater (Waters, Milford, MA, USA).

A Sciex API 3000 mass spectrometer was used as the detector (Sciex, Ont., Canada). Analyst 1.1 (Sciex, Ont., Canada) was used to acquire and evaluate the chromatographic data.

A computer program, named 'LC Model', containing the Band Tracking algorithm was developed in a Delphi7 (Borland, Scotts Valley, CA, USA) environment on a Pentium

III 600 MHz personal computer for evaluating the proposed model. DryLab (Rheodyne, LLC Rhonert Park, CA, USA) was used to compare our results with a conventional prediction model which is referred to as the Linear Solvent Strength, LSS, model.

3.3. Chromatographic conditions

A Symmetry shield column 100 mm × 2.1 mm (length × internal diameter) and 3.5 μm particle size (Waters, Milford, MA, USA) was used for chromatographic separation. Solvent A consisted of a mixture of 0.1% (v/v) of formic acid in purified water and solvent B consisted of 100% acetonitrile. The flow rate was set at 0.2 ml/min.

The mobile phase composition or gradient conditions are indicated in the text.

The injection volume was 10 μl in all cases.

The column heater was set at a temperature of $40 \pm 1\,°C$.

4. Results and discussion

4.1. Experimental design

Initial experiments were carried out to establish the chromatographic behaviour of each analyte. Isocratic chromatograms were recorded to calibrate the Band Tracking Model and for DryLab the LC gradient (two runs) method was used. The dead time t_0 was determined by injecting a 100 ng/ml disodium hydrogen phosphate solution and recording the initial disturbance of the baseline produced by the MS in negative mode. Although a short column can be used for this separation, the length of the column (10 cm) was chosen to demonstrate the prediction capacity of the BT model.

Different gradient conditions were used to compare the experimentally obtained results with the predicted results of both models. Gradient conditions were designed to demonstrate the predictive possibilities of BT model and to demonstrate the differences compared to the LSS model. A description of the programmed gradient curves can be found in Tables 1–6.

Dwell volumes and the dilution volume were measured as mentioned before or as indicated in the DryLab manual for the DryLab program [14].

4.2. Results

The system parameters V_{dwell}, V_d and V_{avg} were determined as discussed before from an UV detector trace.

The dwell volume for the BT model was found to be 0.725 ml and for use with DryLab the dwell volume was found to be 0.930 ml as calculated according to the manual. The V_d and V_{avg} values were found to be 0.240 and 0.300 ml, respectively. V_{dwell}, V_d and V_{avg} are determined once and used as a constant value at each experiment. In our computer program, the gradient curve profile was build with a Δt of 0.005 min (Section 2.3.3.4). This corresponds to V_{res} value of 0.001 ml at a flow of 0.2 ml/min.

The results of the practical and theoretical experiments for five different programmed gradient shapes, gradients a–f, can be found in the corresponding Tables 1–6. A graphical representation of the corresponding predictions of the BT model is given in Fig. 5a–f. In these figures the peaks and the gradient curve as eluted from the column are drawn as predicted by the BT model.

Gradients a and b are straight forward linear gradients. A shift from the programmed curve is observed due to the dwell volume and the dead time, t_0. All peaks elute in the linear part of the curve. Both the BT model and the LSS model lead to good predictions.

Gradient c is a steeper curve and the rounding becomes obvious. The retention times of the first peaks are well pre-

Table 1
Description and results of gradient *a*

Gradient profile A		Comp.	tr exp. (min)	tr BT model (min)	Relative difference (%)	tr LSS model (min)	Relative difference (%)
t (min)	B (%)						
0.0	20	D0	6.26	6.27	0.2	6.24	−0.3
0.1	20	D1	8.40	8.47	0.9	8.41	0.2
10	50	D2	10.36	10.38	0.2	10.38	0.2
11	50	D3	11.468	11.56	0.8	11.49	0.2
11.1	20						

Table 2
Description and results of gradient b

Gradient profile B		Comp.	tr exp. (min)	tr BT model (min)	Relative difference (%)	tr LSS model (min)	Relative difference (%)
t (min)	B (%)						
0.0	20	D0	6.43	6.29	−2.1	6.24	−2.9
0.1	20	D1	8.93	8.84	−1	8.80	−1.4
12	45	D2	11.35	11.35	−1.8	11.47	−0.8
12.1	20	D3	13.02	13.02	−0.5	13.0	−0.2

Table 3
Description and results of gradient c

Gradient profile C		Comp.	tr exp. (min)	tr BT model (min)	Relative difference (%)	tr LSS model (min)	Relative difference (%)
t (min)	B (%)						
0.0	20	D0	6.04	6.09	0.8	6.23	3.1
0.1	20	D1	6.96	7.09	1.9	7.09	1.9
1.5	40	D2	7.77	7.92	1.9	7.56	−2.7
5	40	D3	8.42	8.55	1.6	7.89	−6.3
5.1	20						

Table 4
Description and results of gradient d

Gradient profile D		Comp.	tr exp. (min)	tr BT model (min)	Relative difference (%)	tr LSS model (min)	Relative difference (%)
t (min)	B (%)						
0.0	25	D0	3.98	3.92	−1.5	3.15	−20.9
0.8	25	D1	5.448	5.33	−2.2	4.95	−9.1
0.85	35	D2	7.46	7.43	−0.4	7.36	−1.3
4	35	D3	8.739	8.72	−0.2	8.36	−4.3
4.1	25						

Table 5
Description and results of gradient e

Gradient profile E		Comp.	tr exp. (min)	tr BT model (min)	Relative difference (%)	tr LSS model (min)	Relative difference (%)
i (min)	B (%)						
0.0	20	D0	5.95	5.83	−1.9	6.18	4.0
0.1	20	D1	6.78	6.75	−0.4	6.42	−5.3
0.15	35	D2	7.96	7.88	−1.0	7.16	−10.0
6	35	D3	9.17	8.96	−2.3	8.12	−11.5
6.1	20						

Table 6
Description and results of gradient f

Gradient profile F		Comp.	tr exp. (min)	tr BT model (min)	Relative difference (%)	tr LSS model (min)	Relative difference (%)
t (min)	B (%)						
0.0	20	D0	6.52	6.33	−2.9	5.24	−19.6
2	20	D1	8.51	8.33	−2.1	8.68	2.1
3	40	D2	9.50	9.57	0.7	9.13	−3.9
4	40	D3	10.96	11.04	0.7		
6	20						

dicted by the LSS model and by the BT model as they elute in a more or less linear part of the curve. The third and fourth peaks elute in the rounded part. Here the predictions of both models begin to differ. The later the peak elutes in the flat part of the curve, the larger the difference.

Gradient d consists of an isocratic part and a small step gradient. As the prediction of retention times of pre-eluting peaks is less accurate when using the gradient mode of DryLab [12], we concentrate on the gradient part (the last eluting two peaks). As the gradient step is relatively small and the higher modifier concentration is kept constant for a longer period, the calculated actual gradient profile approximates the programmed block gradient. This results in a smaller difference between the LSS model and the BT model however, the differences in prediction capability is obvious.

Gradient profile e is programmed as a step gradient just after the injection occurred. The initial hold of 0.1 min is inserted to allow the injection mixture to migrate to the column before the gradient starts.

The modifier concentration reaches its maximum after the last peak eluted. All the peaks elute in the upcoming part of the curve. The LSS model, however, expects a fast step during the elution of the first peak and therefore the differences in predictions show that the BT method follows the curvature resulting in much smaller prediction errors.

The last gradient, *f*, is to demonstrate the predictive power of the BT model. A negative gradient is an uncommon phenomenon and DryLab refuses to make predictions. However, the band tracking model gives a good estimation of the resulting curve and the predicted retention times are close to the experimentally obtained results.
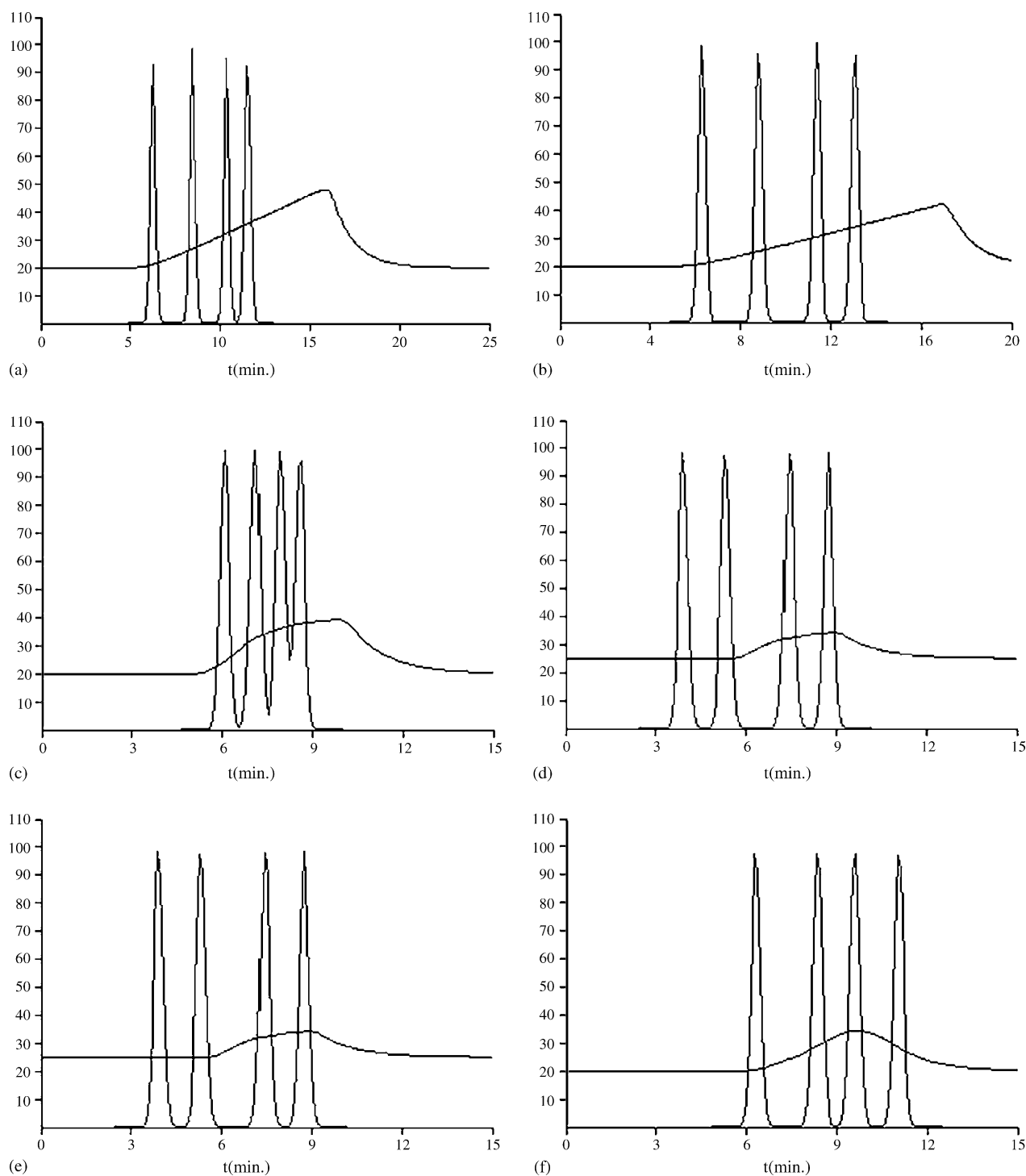
Fig. 5. chromatograms as predicted by the BT model. The *Y*-axis represents the relative peak height and the actual modifier concentration at the end of the column as indicated by the curve. Figures are discussed in the text.

The differences in retention time prediction arise mainly from the rounding of the gradient curve as the largest differences can be observed in these parts of the (predicted) gradient curves. The effect of the use of Eq. (2) was not demonstrated during these experiments.

Although not demonstrated here, the BT model also provided us good prediction results when using different LC equipment, different flow rates or different column geometries using the same values for the parameters V_{dwell}, V_d and V_{avg}.

A detailed description of probable sources of errors of simulation models is given in ref. [12].

From the simulated gradient profile, as can be seen in Fig. 5, a good estimation can be made for the re-equilibration

time of column after the mobile phase condition is set to initial conditions. Re-equilibration is complete as the gradient curve reaches the last programmed modifier concentration, e.g. the initial conditions.

5. Conclusions

The proposed Band Tracking model is able to make retention time predictions with good accuracy. The BT model is able to follow the disturbed curvature of the gradient which is due to dead volumes in the LC system. Therefore, the model is suitable for the use with narrow bore LC-systems. It is a very helpful tool to be used in the development of LC–MS analyses where short run times are preferred. It can be used to determine gradient conditions to separate the analytes from interferences affecting the MS response and to determine the re-equilibration time of the LC system after the mobile phase composition has changed. When using the BT model, reliable predictions can be made using conventional LC equipment and it therefore is can be a good supplement to the existing prediction models.

6. Nomenclature

a_i	migration distance on the column of component i (cm)
Δa	travelled distance of a band during Δt (cm)
A, B, C	retention parameters in the relationship between the modifier concentration and the capacity factor
BT	band tracking, name for the proposed algorithm
F	mobile phase flow (ml/min)
k_i	capacity factor of component i
k^*	momentary capacity factor in the middele of the column during gradient elution
L	column length (cm)
LSS	linear solvent strength
s	gradient slope
t	chromatogram time (min) since start of injection
t_{corr}	time corrected for gradient delay on the column (min)

t_{dwell}	dwell time (min)
t_{start}	start time (min)
t_0	dead time (min)
tr_i	retention time of component i (min)
Δt	small finite time period (min)
v_0	linear mobile phase velocity (cm/min)
v_i	linear velocity of component i (cm/min)
V_d	dilution volume (ml)
V_{avg}	averaging volume (ml)
V_{dwell}	dwell volume (ml)
V_{res}	resolution volume (ml)

Greek letters

α	fractional change in mobile phase composition
φ	modifier concentration (%)
φ_0	modifier concentration at start time (%)
φ_n	succeeding modifier concentration (%)
$\varphi_{(t)}$	modifier concentration at time t (%)

References

[1] I. Molnar, J. Chromatogr. A 965 (2002) 175.
[2] A. Smidt, I. Molnar, J. Chromatogr. A 948 (2002) 51.
[3] L. van Heukelem, C.S. Thomas, J. Chromatogr. A 910 (2002) 31.
[4] L.R. Snyder, in: Cs. Horváth (Ed.), High Performance Liquid Chromatography. Advances and Perspectives, vol. I, Academic press, New York, 1980, chapter 4.
[5] J.W. Dolan, L.R. Snyder, J. Chromatogr. A 799 (1998) 21.
[6] C. Horváth, W. Melander, I. Molnar, J. Chromatogr. 125 (1976) 129.
[7] L. Romananyshyn, P.R. Tiller, P. Alvaro, A. Pareira, C.E.C.A. Hop, Rapid commun. Mass spectrom 15 (2001) 313.
[8] W. Longxing, Z. Lefeng, X. Hongbin, L. Xinmiao, Anal. Chim. Acta 476 (2003) 123.
[9] P. Schoenmakers, H.A.H. Billiet, L. de Galan, J. Chromatogr. 185 (1979) 179.
[10] R.S. Hodges, J.M.R. Parker, C.T. Mant, R.R. Sharma, J. Chromatogr. 458 (1988) 147.
[11] A.P. Bruins, T.R. Covey, J.D. Henion, Anal. Chem. 59 (1987) 2642.
[12] J.W. Dolan, L.R. Snyder, R.G. Wolcott, P. Haber, T. Baczek, R. Kaliszan, L.C. Sander, J. Chromatogr. A 857 (1999) 41.
[13] L. Snyder, J.L. Glajch, J.J. Kirkland, Practical HPLC Method Development, Wiley-Interscience, 1988.
[14] DryLab manual, Rheodyne, Rhonert Park, CA, USA.
[15] M.A. Quarry, R.L. Grob, L.R. Snyder, J. Chromatogr. 285 (1984) 1.
[16] D.D. Lisi, J. Stuart, L. Snyder, J. Chromatogr. 155 (1991) 1.